Fuel xxx (2014) xxx–xxx

Contents lists available at ScienceDirect

Fuel

journal homepage: www.elsevier.com/locate/fuel

Modeling and analysis of the pyrolysis of bio-oil aqueous fraction in a fixed-bed reactor

Shaomin Liu [a,*], Lei Chu [a], Mingqiang Chen [b], Wentao Zhang [b], Wenping Xin [a]

[a] School of Earth Science and Environmental Engineering, Anhui University of Science and Technology, Huainan 232001, PR China
[b] School of Chemical Engineering, Anhui University of Science and Technology, Huainan 232001, PR China

HIGHLIGHTS

- The thermodynamic parameters and mass and heat balance equation were estimated.
- A mathematical model on the pyrolysis of bio-oil was established.
- The effects of temperature on the pyrolysis of bio-oil aqueous fraction were studied.
- The comparison of the established model and the experimental results was performed.

ARTICLE INFO

Article history:
Received 31 December 2013
Received in revised form 1 May 2014
Accepted 5 May 2014
Available online xxxx

Keywords:
Bio-oil
Fixed-bed reactor
Pyrolysis
Reaction kinetics
Mathematic model

ABSTRACT

The pyrolysis of bio-oil is important in improving the utilization of biomass energy and the environmental protection. In this study, simulations were conducted in the Aspen Plus environment using the Gibbs reactor to simulate the equilibrium compositions of the bio-oil pyrolysis products at different temperatures. The molar heat capacity at constant pressure of the chemical balance system was calculated through simulation. The thermodynamic parameters of the reactor were determined using the thermodynamic equations and the mass balance principle. Furthermore, the temperature distribution and conversion rate of different catalyst beds were calculated by combining the Runge–Kutta method with the Matlab software. Finally, experiments were performed in a fixed bed reactor, and the experimental results were compared with the simulated results. The calculation result of the established model is in good agreement with the experimental results.

1. Introduction

Bio-oil has much higher energy volume density than solid biomass and poses a great solution to the problem that biomass raw materials are hard to be massively collected, stored, or transported [1–3]. It can be separated into oil phase and aqueous phase by adding water. Due to the lack of fossil fuel resources and the growing greenhouse effect, the utilization of bio-oil as a potential fuel substitute can satisfy the human society's need for energy with wide application prospect [4–6]. Bio-oil can be used directly as low level fuels to provide heat or generate power, or used in internal engine after upgrade.

The pyrolysis of bio-oil is the initial stage of its combustion and gasification, and therefore has a key function in the thermochemical use of bio-oil and the in-depth investigation of pyrolysis characteristics. The kinetics of bio-oil is important [7,8]. Numerous systematic studies on the pyrolysis characteristics and effects of operating conditions on the product distribution have been carried out [9–14]. The main pyrolysis products are water, permanent gases, and char. The yield and the composition of the pyrolysis products depend on the type of reactor, reactor temperature, and catalysis. However, the pyrolysis characteristics of crude bio-oil components have had some issues, such as coke formation and low heating value. Numerous studies have been reported [15,16]; nevertheless, few studies have reported on the comprehensive mass and molar balances at high temperature in a fixed bed [17–19]. The mathematical description relative to the pyrolysis of bio-oil has not been fully understood. A great deal of interest has been addressed to the utilization of bio-oil aqueous fraction; however, the mathematical model of the pyrolysis of bio-oil aqueous fraction has rarely been studied.

This study aims to determine the pyrolysis product yields and the pyrolysis mathematical model to provide significant data for the design and optimization of related gasification and combustion

* Corresponding author. Tel./fax: +86 554 6668742.
E-mail address: shmliu1@163.com (S. Liu).

http://dx.doi.org/10.1016/j.fuel.2014.05.001
0016-2361/

Please cite this article in press as: Liu S et al. Modeling and analysis of the pyrolysis of bio-oil aqueous fraction in a fixed-bed reactor. Fuel (2014), http://dx.doi.org/10.1016/j.fuel.2014.05.001

reactors. Moreover, data from this study would provide some theoretical basis for further studies on the use of bio-oil.

In this study, simulations were conducted in the Aspen Plus environment using the Gibbs reactor to simulate the equilibrium compositions of the bio-oil pyrolysis products at different temperatures. The molar heat capacity at constant pressure of the chemical balance system was calculated through simulation. The thermodynamic parameters of the reactor were determined using the thermodynamic equations and the mass balance principle. Finally, the temperature distribution and conversion rate of different catalyst beds were calculated by combining the Runge–Kutta method with the Matlab software.

2. Materials and methods

2.1. Experimental materials

The bio-oil used for thermal analysis was obtained by the pyrolysis of wheat stalk in a small-scale fixed-bed reactor in our laboratory. The sample was prepared by mixing the bio-oil and distilled water. The mass ratio of the distilled water to bio-oil was 4. The water phase of the mixture was used for the thermal analysis.

In this work, acid-activated attapulgite catalyst was used as the support for nickel oxide and molybdenum oxide and simple precipitation was utilized to establish them on the acidized attapulgite. The diameters of the catalyst particles were 1–2 mm; the height of the catalytic bed was 10 cm; the bio-oil feed rate was 2 mL/min to 10 mL/min; the density ρ_B of the bed was 562.39 kg/m^3, the porosity of the catalyst was $\varepsilon = 0.754$; the empty bed mass velocity of the fluid was $G = 76.394$ kg/(m^2 h).

Fig. 1 presents the bio-oil catalytic pyrolysis reactor. The reactor is made of heat-resistant stainless steel tube with a 100 mm diameter and an 800 mm length (including the upper and bottom heads). The reaction temperature is controlled by electronic heating and thermostat. The bio-oil and steam enter the reactor from the upper nozzle. The generated gas is led at different positions on the side face of the reactor for the real-time composition test. The residual product is separated at the bottom of the reactor. The reactor is relatively larger than the catalyst particles, and the height of the bed is over 100 times of the diameters of the particles. The ratio of the diameter of the reactor to that of the catalyst particles is larger than 10. Investigation shows that when the bed height is 100 times over the particles' diameter, the influences of the axial diffusion, thermal conductivity, and radial velocity distribution on the conversion rate are negligible.

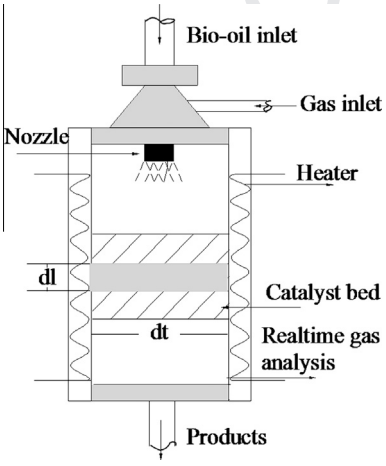

Fig. 1. Catalytic pyrolysis reactor.

2.2. Experimental methods

The catalytic pyrolysis of bio-oil is an endothermic reaction with moderate thermal effect and reaction speed rate. The diameter and bed height of the fixed-bed reactor are significantly larger than that of the catalyst particles, respectively. Therefore, the tubular fixed-bed reactors with thin and long tubes and high flowing rate can be treated as plug-flow or pseudo-homogeneous reactors. In this study, a pseudo-homogeneous, one-dimensional, and plug flow model was selected according to the characteristics of the tubular fixed-bed reactors and the applicable conditions of each model. Combining the features and thermodynamic parameters of bio-oil, the pyrolysis reaction temperatures and the conversion rate distribution of the catalytic bed of the reactor were investigated to determine the key parameters of the reactor.

The bio-oil used for pyrolysis was obtained through fast pyrolysis of pine wood sawdust in a small scale fixed bed at 500 °C. The sample was prepared by mixing the bio-oil and distilled water. The water phase of this mixture was used for thermal analysis. The elemental composition and properties of the bio-oil are shown in Table 1.

Table 1 indicates that the bio-oil aqueous fraction mainly consists of light component organic compounds, which mostly contain carbohydrate-derived compounds. The high viscosity of bio-oil aqueous fraction leads to a bad fluidity low heating value because of the high oxygen content. The basic chemical formula of the water-soluble fractions in bio-oil can be represented by $C_nH_mO_z$. The chemical formula of the bio-oil aqueous fraction can be described by $C_{2.49}H_{9.93}O_{3.73}$, based on the elementary composition.

According to the specific situation of the studied reactor, the establishment of the model is based on the following assumptions:

(1) The property and velocity of the fluid at the cross section perpendicular to the direction of the fluid flow are uniform; velocity, temperature, and concentration gradients do not exist at the radial direction.
(2) The axial thermal and mass transfer is caused by the overall plug flow only.
(3) No radial velocity distribution or axial dispersion of the bed exists at the direction perpendicular to the flow direction.

The outcome of reaction is congealed and separated into the gas and liquid phases. After being dried with non-condensable gas, the gaseous product was determined using GC. The liquid phase was determined using GC–MS. The liquid content was determined using a moisture analyzer, and carbon deposition was determined using TG.

The maximum stoichiometric hydrogen yield can be described by the following reaction stoichiometry (complete pyrolysis of bio-oil aqueous fraction):

$$C_nH_mO_z + (2n - z)H_2O \rightarrow nCO_2 + (2n + m/2 - z)H_2 \quad (1)$$

According to the Eq. (1), the mole ratio of H_2 obtained to stoichiometric H_2 is defined as hydrogen yield, which is calculated as Eq. (2):

$$Y(H_2) = \frac{\text{moles of } H_2 \text{ obtained}}{\text{moles of } H_2 \text{ in stoichiometric potential}} \times 100\% \quad (2)$$

The mole ratio of CH_4 (CO, CO_2) obtained to the carbon in the feed is defined as CH_4 (CO, CO_2) yield and the CH_4 (CO, CO_2) yield is calculated by Eq. (3) [20]:

$$Y(CH_4, CO, CO_2) = \frac{\text{moles of } (CH_4, CO, CO_2) \text{ obtained}}{\text{moles of carbon in the feed}} \times 100\% \quad (3)$$

Please cite this article in press as: Liu S et al. Modeling and analysis of the pyrolysis of bio-oil aqueous fraction in a fixed-bed reactor. Fuel (2014), http://dx.doi.org/10.1016/j.fuel.2014.05.001

Table 1
Elemental composition and basic properties of bio-oil.

Sample	C (w/%)	H (w/%)	O (w/%)	N (w/%)	S (w/%)	Water (w/%)	Kinematic viscosity CST (313 K)	pH	HHV (MJ/kg)
Bio-oil	29.86	9.95	59.728	0.405	0.067	44.21	2.84	3.01	19.3

Carbon element takes up 29.86% of the bio-oil weight and the increase in carbon conversion in the gaseous product represents the decrease in carbon loss in the form of char. The carbon conversion of gas product is calculated by Eq. (4):

$$\text{Carbon conversion}(\%) = \frac{\text{moles of carbon of gas production}}{\text{moles of carbon in the feed}} \quad (4)$$

2.2.1. Dynamic equations

The composition of bio-oil is complex; thus, the pyrolysis kinetics analysis of bio-oil usually focuses on the overall reaction of all of the components. The first-order reaction is often used in previous studies to describe the dynamic parameters of the bio-oil's volatilizing and combusting stages [21,22]. To improve the reliability of result analysis and obtain the optimal reaction mechanism, 30 reaction mechanism functions given by [23] were adopted in the present study for the preliminary investigation. The dynamic parameters of the pyrolysis of bio-oil were analyzed using the Achar differential and Coats–Redfern integral methods.

Based on the previous results [23], the kinetic equations can be defined as follows:

$$\frac{d\alpha}{dT} = \frac{3}{2} A \exp(-E/RT)(1+\alpha)^{2/3}[(1+\alpha)^{1/3} - 1]^{-1}. \quad (5)$$

2.2.2. Mass and heat balance equation

With bio-oil aqueous fraction as raw material, in the plug-flow reactor for isothermal reaction, the component of the material changes from one section to the other along the flow direction of the reactor was investigated. As shown in Fig. 1, when a micro control body with a length of L and a volume of dV was selected randomly for the mass and heat balance calculation in the fixed-bed reactor, the feeding amount was equal to the sum of the ejection and accumulation amounts.

The reactor in the experiment uses an electronic heating mantle; the heat loss of which is not considered. The value of the heat provided in the bed is constant from the top to the bottom, which is the value of the heat provided by a unit surface area of the bed. The external heat provided equals to the heat required by the temperature increase and the fluid reaction. The equation of the mass and heat balance of the material is calculated using the following equations:

$$F_0 dx = \rho_B(-r)dV_R, \quad (6)$$

$$Q\pi d_t dl = G\frac{\pi}{4} d_t^2 c_p dT + F_0 dx(-\Delta H). \quad (7)$$

The reaction kinetics equation can be simplified to

$$(-r) = f(x,T). \quad (8)$$

The following equation is obtained by combining Eq. (6) with Eqs. (7) and (8);

$$\frac{dx}{dl} = \rho_B \frac{(-r)}{G}\overline{M}, \quad (9)$$

$$\frac{dT}{dl} = -\frac{\rho_B(-r)(-\Delta H)}{Gc_p} + Q. \quad (10)$$

The boundary conditions are $l = 0.2$, $x_0 = 0.1$, and $T = 50$ °C.

In the above equations, G is the empty bed mass velocity of the fluid (kg/(m^2 h)); ρ_B is the catalyst bulk density (kg/m^3); Q is the external heat of the unit area (kJ/(m^2 h)); $-r$ is the reaction rate (kmol/h); C_p is the heat capacity (kJ/(kg °C)); $\overline{M}$ is the average molecular weight of the material at any direction (kg/kmol); ΔH is the reaction heat (kJ/kmol); l is the distance at the reactor length direction (m).

2.2.3. Estimation of the thermodynamic parameters

For the reaction system of the reactor, heat capacity and reaction heat are the functions not only of temperature but also composed by the system. The system composition could be connected with temperature through the reaction dynamic equation. Therefore, heat capacity and reaction heat are actually the single-variable functions of temperature [24,25].

The molar heat capacity at constant pressure of the reaction system under different temperatures was adopted in this study. Through the fitting of the polynomial function, based on the correlation of physics and chemicals, the pure components of the gasification product of bio-oil, and the temperature, the heat capacity of the reaction system has the similar relationship to temperature.

Although bio-oil is a mixture, a study has shown that bio-oil also has similar expression as follows [26]:

$$C_P = 0.00882T - 0.13073. \quad (11)$$

The balance composition of the products of bio-oil under different temperatures can be simulated using the Gibbs reactor of Aspen plus. Through the major reaction equations of the bio-oil's thermal decomposition, the heat capacity of the reaction system can be treated as the added value of the heat capacities calculated by several thermal decomposition reactions. Finally, the molar heat capacities at constant pressure at different temperatures can be obtained.

2.2.4. Mathematical model of the reactor

For the reaction heat and the average molar mass of the reaction system at the different position of the reactor, they could be calculated using similar methods. The thermodynamic parameters of bio-oil, such as the molar heat capacity at constant pressure, average molar mass, and reaction heat at different temperatures are respectively expressed by the following equations [26]:

$$Cp = 3210.14 - 34.465T + 0.122T^2 - 8.931 \times 10^{-5}T^3, \quad (12)$$

$$M = 22.355 + 0.006T - 1.3 \times 10^{-5}T^2 - 1.88 \times 10^{-8}T^3, \quad (13)$$

$$\Delta H = 92220.15 - 650.966T + 1.64T^2 - 0.001T^3. \quad (14)$$

The molar heat capacity at constant pressure, average molar mass, and reaction heat at different temperatures are listed in Table 2. It can be seen in Table 2 that the molar heat capacity increases as the temperature increases, however, the average molar mass decreases gradually and it was inversely proportional at higher temperature range. In addition, the reaction heat first decreased at a temperature range of 323.15–503.15 K and then increased dramatically as the temperature increases at the temperature range from 503.15 K to 863.15 K.

After substituting Eqs. (5), (12), (13), and (10) into Eqs. (9) and (10), the following formulas are obtained. The differential equation set formed by Eqs. (15) and (16) is the mathematical model for the

Please cite this article in press as: Liu S et al. Modeling and analysis of the pyrolysis of bio-oil aqueous fraction in a fixed-bed reactor. Fuel (2014), http://dx.doi.org/10.1016/j.fuel.2014.05.001

Table 2
Molar heat capacity, average molar mass, and heat of reaction at different temperatures.

T (K)	Cp (J/mol K)	M (kg/kmol)	ΔH (kJ/kmol)
323.15	935.77	22.76	64,200
383.15	983.32	22.76	25,300
443.15	1032.33	22.74	21,100
503.15	1091.99	22.66	20,900
563.15	1223.06	22.46	23,000
623.15	1624.07	22.44	28,100
683.15	2649.31	21.30	37,400
743.15	4592.94	20.19	51,900
803.15	6958.06	18.70	71,700
863.15	8050.40	17.03	94,400

calculation of the designing parameters of the reactor. The initial conditions are $l = 0.2$, $x_0 = 0.1$, and $T = 50$ °C.

$$\frac{d\alpha}{dl} = 76.362 \times r \times M \tag{15}$$

$$\frac{dT}{dl} = 76.362 \times r \times \Delta H + 592.391 \times C_P \times (T - T_0) \tag{16}$$

In the above equations, r is the reaction rate (kmol/h); M is the average molecular weight of a material at any direction (kg/kmol); ΔH is the reaction heat (kJ/kmol); C_P is the molar constant pressure heat capacity (kJ/(kg °C)); T is the gas temperature; T_0 is the catalytic bed temperature.

3. Results and discussion

3.1. Effect of the reaction temperature on the simulated results

Fig. 2 presents the experimental results when the catalyst particles have a diameter of 2–3 mm, the bio-oil weight hourly space velocity (WHSV) was 1.8 h^{-1}, and the moisture of bio-oil was 40%. The simulated results are also shown in Fig. 2. The yield of H_2 and CO rapidly increased at a temperature range of 500–700 °C; however, the increasing trend became gradual when the temperature was beyond 750 °C. The molar percentage of H_2 and CO reached 32% and 50%, respectively, when the temperature reached 750 °C. On the contrary, the molar percentage of CH_4 decreased from 19.7% to 0.78% when the temperature ranged from 500 °C to 900 °C. The curve tendency of the CO_2 molar percentage was similar to that of CH_4 because the gasification of bio-oil aqueous fraction was completely converted and the corresponding CO_2 content can be obtained. At the same time, the carbon and bio-oil conversions also increased with the increase in temperature. The tendency plateaus and the conversion of carbon and bio-oil became steady when the temperature was beyond 750 °C. The pyrolysis of bio-oil is an endothermic reaction; thus, the increase in temperature is conducive to the reaction. Fig. 2 shows that temperature has an important function in increasing the H_2 yield during the pyrolysis of bio-oil in a fixed-bed reactor. The pyrolysis reaction can be divided into the evaporation stage of volatile fractions and the decomposition stage of heavy fractions. Low reaction temperature favors the decomposition of heavy fractions. Simultaneously, the increase in carbon conversion in the gaseous product represents the decrease in carbon loss in the form of char. High reaction temperature promotes the water–gas shift reaction, where higher productivity of H_2 and CO occurs. Therefore, considering the electrical expenditure caused by the rise in temperature, the favorable reaction temperature is 700–800 °C.

3.2. Effect of the reaction temperature on the experimental results

The pyrolysis experiment of bio-oil aqueous fraction was conducted in a fixed-bed reactor under the same conditions as those of the simulation. The results of the effect of reaction temperature on the composition of the gaseous product of the pyrolysis of aqueous fractions in bio-oil are given in Fig. 3. The yield curve tendency of CO_2, CO, H_2, and CH_4, as well as the conversion curve tendency of carbon and bio-oil, is similar to that of the simulated results. The molar percentage of H_2 and CO increased with the increase in reactor temperature. The molar percentages of CH_4 and CO_2 were characterized with a converse changing trend against those of H_2 and CO. The yield of each gaseous product became nearly constant as the temperature increased from 700 °C to 750 °C. The experimental results also indicated that high temperature can help increase the yield of pyrolysis products.

3.3. Comparison between simulation and experiment

The differential equation set formed by Eqs. (5), (12), (13), (10), (15), and (16) needs to be solved by numerical calculating method. The Runge–Kutta method combined with the Matlab software was used to solve the equation. The temperature and conversion rate distribution attributes can be obtained after the calculation. The experiment was conducted with a catalyst bed of 25 cm at a reac-

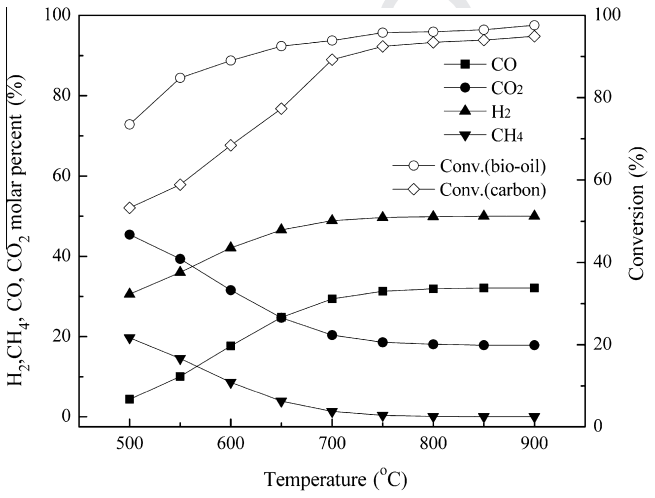

Fig. 2. Simulated results of pyrolysis of bio-oil in a fixed bed.

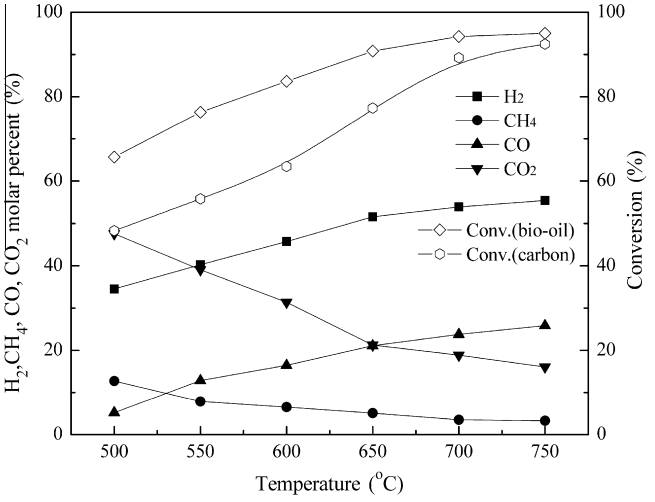

Fig. 3. Experimental results of pyrolysis of bio-oil in a fixed bed.

Please cite this article in press as: Liu S et al. Modeling and analysis of the pyrolysis of bio-oil aqueous fraction in a fixed-bed reactor. Fuel (2014), http://dx.doi.org/10.1016/j.fuel.2014.05.001

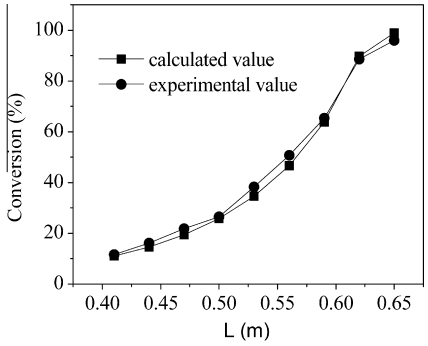

Fig. 4. Comparison of conversion between simulation and experiment.

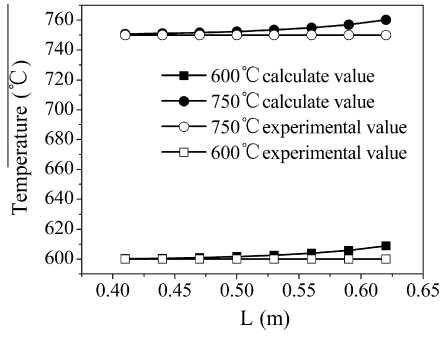

Fig. 5. Comparison of temperature field between simulation and experiment.

tion temperature of 750 °C and a WHSV of 1.2 h^{-1}. The experimental and model values are shown in Figs. 4 and 5.

The result of the catalytic pyrolysis experiment in the catalyst bed at 0.4–0.65 m of the middle of the reactor, as shown in Fig. 4, indicates that the length of the reactor significantly influenced the bio-oil catalytic pyrolysis for H_2 production. The conversion rate of bio-oil gradually increased with the increase in reactor length. At the middle 0.4–0.6 m of the reactor where the catalyst is placed, the conversion of bio-oil rapidly increased. At a 0.22 m catalytic bed length, the conversion of bio-oil was up to 90%. Therefore, the optimum catalytic bed length is 0.2–0.25 m.

During the experiment, the conversion rate of bio-oil at the upper end of the reactor was slightly higher than the calculated value of the model, which may because the catalyst was placed at the reactor middle and the catalytic pyrolysis effect happened at the surface of the catalyst bed. The conversion rate of bio-oil at the back end of the reactor was slightly lower than the calculated value, which may be because the bio-oil at this reaction length was not completely converted. The experimental conversion rate of the whole catalyst bed does not significantly differ from the calculated value.

Fig. 4 also shows that the conversion rate of bio-oil at the upper end of the reactor was low and the conversion mainly occurred at the catalyst bed section. The reason is probably that the transform reaction of bio-oil occurred at the upper end of the reactor after being heated. In addition, the catalytic pyrolysis occurred at the surface of the catalyst bed, which accelerated the conversion of the bio-oil molecules.

Fig. 5 presents the catalytic pyrolysis experiment at a temperature of 750 °C and the simulation of the relationship between the reactor length and the temperature change through calculation. With the change of the reaction length, the influence of the reaction temperature decreased. As the fixed-bed reactor was heated by a temperature controller, the experimental temperature remained at 600 and 750 °C during the experiment. At the upper end of the reactor, the steam transforming and the bio-oil molecule endothermic reactions occurred; at the middle section of the reactor, the experimental value was consistent with the model value; and at the back end, the catalytic pyrolysis reaction was an exothermic reaction, which slightly increased the model calculated temperature.

4. Conclusions

In this study, the mass and heat balance equations and the thermodynamic parameters were estimated. A mathematical model on the pyrolysis of bio-oil was established. Temperature is important for the pyrolysis of bio-oil aqueous fraction for hydrogen production. High temperature can help increase the yield of H_2 and CO, as well as reduce the rate of carbon deposition. The favorable reaction temperature is 700–800 °C. The length of the reactor significantly influenced the catalytic pyrolysis for bio-oil, with the optimum catalytic bed length being 0.2–0.25 m. The simulated value of the conversion is in good agreement with the experimental results.

Acknowledgments

This research project was financially supported by: National 863 Foundation (2014BAD02B03), the National Natural Science Foundation of China (No. 21376007), Anhui Natural Science Foundation (KJ2012A070), Young and Middle-Aged Academic Key Members of Anhui University of Science and Technology, National Undergraduate Innovation Training Program (201210361004).

References

[1] Salehi E, Abedi J, Harding T. Bio-oil from sawdust: effect of operating parameters on the yield and quality of pyrolysis products. Energy Fuels 2011;25:4145–54.
[2] Bridgwater AV. Principles and practice of biomass fast pyrolysis processes for liquids. J Anal Appl Pyrol 1999;51:3–22.
[3] Mullen CA, Boateng AA. Chemical composition of bio-oils produced by fast pyrolysis of two energy crops. Energy Fuels 2008;22:2104–9.
[4] Azad FS, Abedi J, Salehi E, Harding T. Production of hydrogen via steam reforming of bio-oil over Ni-based catalysts: effect of support. Chem Eng J 2012;180:145–50.
[5] Iojoiu EE, Domine ME, Davidian T, Guilhaume N, Mirodatos C. Hydrogen production by sequential cracking of biomass-derived pyrolysis oil over noble metal catalysts supported on ceria-zirconia. Appl Catal A: Gen 2007;323:147–61.
[6] Chen M, Qi X, Wang J, Chen M, Min F, Liu S, et al. Catalytic characteristics and kinetic modeling of cotton stalk pyrolysis. J Fuel Chem Technol 2011;7:585–9.
[7] Lee YK, Kima YS, Ahn JG, Son IH, Shin WC. Hydrogen production from ethanol over Co/ZnO catalyst in a multi-layered reformer. Int J Hydrogen Energy 2010;35:1147–51.
[8] Wu C, Huang Q, Sui M, Yan Y, Wang F. Hydrogen production via catalytic steam reforming of fast pyrolysis bio-oil in a two-stage fixed bed reactor system. Fuel Process Technol 2008;89:1306–16.
[9] Masakazu SA, Watkinson P, Ellis N. Steam gasification reactivity of char from rapid pyrolysis of bio-oil/char slurry. Fuel 2010;89:3078–84.
[10] Meng X, Xu C, Li L, Gao J. Kinetics of catalytic pyrolysis of heavy gas oil derived from canadian synthetic crude oil. Energy Fuels 2011;25:3400–7.
[11] Wang CW, Yin XL, Wu CZ, Ma LL, Zhou ZQ, Xie JJ. Kinetics of pyrolysis of bio-oil and its heavy fractions. J Eng Thermophys 2009;30:1783–6.
[12] Kok MV. Thermal behavior and kinetics of crude oils at low heating rates by differential scanning calorimeter. Fuel Process Technol 2012;96:123–7.
[13] Branca C, Di Blasi C, Russo C. Devolatilization in the temperature range 300–600 K of liquids derived from wood pyrolysis and gasification. Fuel 2005;84:37–45.
[14] Shahla S, Ngoh GC, Yusoff R. The evaluation of various kinetic models for base-catalyzed ethanolysis of palm oil. Bioresour Technol 2012;104:1–5.
[15] Sommarive S, Grana R, Maffei T, Pierucci S, Ranzi E. A kinetic approach to the mathematical model of fixed bed gasifiers. Comput Chem Eng 2011;35:928–35.
[16] Chhiti Y, Salvador S, Commandré JM, Broust F. Thermal decomposition of bio-oil: focus on the products yields under different pyrolysis conditions. Fuel 2012;102:274–81.
[17] Vaezi M, Passandideh-Fard M, Moghiman M, Charmchi M. Gasification of heavy fuel oils: a thermochemical equilibrium approach. Fuel 2011;90:878–85.

Please cite this article in press as: Liu S et al. Modeling and analysis of the pyrolysis of bio-oil aqueous fraction in a fixed-bed reactor. Fuel (2014), http://dx.doi.org/10.1016/j.fuel.2014.05.001

[18] Marklund M, Tegman R, Gebart R. CFD modelling of black liquor gasification: identification of important model parameters. Fuel 2007;86:1918–26.
[19] Ashizawa M, Hara S, Kidoguchi H. Gasification characteristics of extra-heavy oil in a research-scale gasifier. Energy 2005;30:2194–205.
[20] Vagia EC, Lemonidou AA. Thermodynamic analysis of hydrogen production via steam reforming of selected components of aqueous bio-oil fraction. Int J Hydrogen Energy 2007;32:212–23.
[21] Chen TJ, Wu C, Liu RH. Steam reforming of bio-oil from rice husks fast pyrolysis for hydrogen production. Bioresour Technol 2011;102:9236–40.
[22] Liu S, Chen M, Hu Q, Wang J, Kong L. The kinetics model and pyrolysis behavior of the aqueous fraction of bio-oil. Bioresour Technol 2013;129:381–6.
[23] Liu S, Chen M, Chu L, Yang Z, Zhu C, Wang J, et al. Catalytic steam reforming of bio-oil aqueous fraction for hydrogen production over Ni–Mo supported on modified sepiolite catalysts. Int J Hydrogen Energy 2013;38:3948–55.
[24] Garcia PM, Chaala A, Pakdel H, Kretschmer D, Roy C. Characterization of bio-oils in chemical families. Biomass Bioenergy 2007;31:222–42.
[25] Park SS, Seo DK, Lee SH, Yu T, Hwang J. Study on pyrolysis characteristics of refuse plastic fuel using lab-scale tube furnace and thermogravimetric analysis reactor. J Anal Appl Pyrol 2012;97:29–38.
[26] Cheng W, Xie K, Zhao R, Zhu X. Research of biomass-oil vapor–liquid phase equilibrium and specific heat-capacity. J Eng Thermophys 2010;31:24–7.

Please cite this article in press as: Liu S et al. Modeling and analysis of the pyrolysis of bio-oil aqueous fraction in a fixed-bed reactor. Fuel (2014), http://dx.doi.org/10.1016/j.fuel.2014.05.001